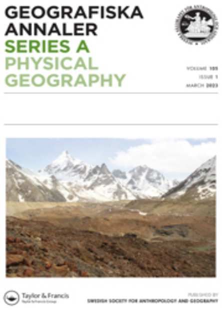

Taylor & Francis
Taylor & Francis Group

Geografiska Annaler: Series A, Physical Geography

ISSN: (Print) (Online) Journal homepage: www.tandfonline.com/journals/tgaa20

Climate indices as predictors of global soil organic carbon stocks

Qin Zhang, Chuixiang Yi, Georg Wohlfahrt, Deliang Chen, Max Rietkerk, Zhenkun Tian, Mousong Wu, Eric Kutter, Jianxu Han, George Hendrey & Shiguo Xu

To cite this article: Qin Zhang, Chuixiang Yi, Georg Wohlfahrt, Deliang Chen, Max Rietkerk, Zhenkun Tian, Mousong Wu, Eric Kutter, Jianxu Han, George Hendrey & Shiguo Xu (15 Apr 2024): Climate indices as predictors of global soil organic carbon stocks, Geografiska Annaler: Series A, Physical Geography, DOI: 10.1080/04353676.2024.2335000

To link to this article: https://doi.org/10.1080/04353676.2024.2335000

Published online: 15 Apr 2024.

GEOGRAFISKA ANNALER: SERIES A, PHYSICAL GEOGRAPHY
https://doi.org/10.1080/04353676.2024.2335000

Climate indices as predictors of global soil organic carbon stocks

Qin Zhang[a], Chuixiang Yi[b,c], Georg Wohlfahrt[d], Deliang Chen[e], Max Rietkerk[f], Zhenkun Tian[b,g], Mousong Wu[h], Eric Kutter[i], Jianxu Han[a], George Hendrey[b,c] and Shiguo Xu[a]

[a]Institution of Water and Environment Research, Dalian University of Technology, Dalian, People's Republic of China; [b]School of Earth and Environmental Sciences, Queens College, City University of New York, New York, NY, USA; [c]Earth and Environmental Sciences Department, Graduate Center, City University of New York, New York, NY, USA; [d]Institut für Ökologie, Universität Innsbruck, Innsbruck, Austria; [e]Department of Earth Sciences, University of Gothenburg, Gothenburg, Sweden; [f]Copernicus Institute of Sustainable Development, Utrecht University, TC Utrecht, The Netherlands; [g]School of Applied Technology, China University of Labor Relations, Beijing, People's Republic of China; [h]International Institute for Earth System Science (ESSI), School of Geography and Ocean Science, Nanjing University, Nanjing, People's Republic of China; [i]Barry Commoner Center for Health & the Environment, Queens College, City University of New York, Flushing, USA

ABSTRACT

Global soils store more carbon than the atmosphere and terrestrial vegetation combined, with a significant proportion located in colder regions. Earth system models incorporating climate-carbon feedback suggest that a warming climate can potentially destabilize soil carbon storage, leading to carbon release into the atmosphere. However, existing models are based on limited measurements of soil organic carbon (SOC) loss and a comprehensive global-scale climate indices that effectively characterizes climate-SOC relationships is currently lacking. In this study, we present a synthetic analysis that evaluates the effectiveness of different climate indices in estimating SOC stocks using a global compilation of SOC data and the Boltzmann Sigmoidal Model (BSM). Our findings reveal that a climate index, defined as TD-Index $= \exp(-0.002T - 0.8D)$, where T and D are mean century temperature (MCT) and dryness respectively, serves as the most reliable predictor for SOC stocks. Furthermore, we observed temperature tipping points for SOC, ranging from −4.5 to −3°C for different soil layers. As the temperature transitions from being below to above the tipping point, the SOC shifts from a stable, high state to a rapid decline. An analysis of the projected temperatures for SOC under various future greenhouse gas emissions scenarios showed a northward shift in the northern hemisphere, potentially opening up vast areas of arctic territory to increased SOC loss from the soils, with corresponding emissions of the stored carbon into the atmosphere. Our findings open up new avenues for research on and management strategies for climate-related SOC dynamics.

ARTICLE HISTORY
Received 1 September 2023
Revised 17 March 2024
Accepted 22 March 2024

KEYWORDS
Soil organic carbon; Boltzmann Sigmoidal Model; future projections; climate indices; carbon-temperature patterns

1. Introduction

The net release of organic carbon from soils (SOC) in the form of carbon dioxide (CO_2) into the atmosphere is the result of the imbalance between organic matter input, primarily driven by plant primary productivity, and respiration by soil microorganisms and plant roots (Crowther

CONTACT Chuixiang Yi cyi@qc.cuny.edu School of Earth and Environmental Sciences, Queens College, City University of New York, Flushing; 11367, USA

et al. 2019; Varney et al. 2020). SOC turnover largely determines the direction and magnitude of climate-carbon cycle feedbacks (Cox et al. 2000; Friedlingstein et al. 2006; Clarke et al. 2021). SOC losses are the result of a complex interplay of factors and cannot be solely attributed to temperature increases (Post et al. 1982; Yi et al. 2010; Luo et al. 2017; Hartley et al. 2021). Predicting SOC losses induced by warming presents uncertainties due to the nonlinear nature of multiple control parameters, whose combined effects do not simply sum up (Wiesmeier et al. 2019).

Although laboratory and field observations have significantly advanced our understanding of the environmental factors influencing SOC losses (Doetterl et al. 2015; Melillo et al. 2017; Crowther et al. 2019; Nottingham et al. 2020), these approaches are often specific to particular soil types and limited in duration, and thus struggle to reveal the bigger picture at larger temporal and spatial scales (Wiesmeier et al. 2019). Besides, the drivers of SOC take distinct weight on various scales, e.g. while soil physico-chemistry is the core factor influencing SOC on the micro scale, at regional and sub-continental scale SOC dynamics are mainly driven by land use and vegetation, and climate is usually the determining variable on a global scale (Doetterl et al. 2015; Wiesmeier et al. 2019). At small spatial scales, where factors such as climate are less variable, the physico-chemical properties of the soil and microbiological factors become important. Whereas at global scales, climate determines the balance of SOC inputs and outputs.

Processes in soil are slow and their responses to environmental factors are not synchronized. The turnover time of SOC varies widely across different soil types (labile or recalcitrant) and depths (Koven et al. 2017; Abramoff et al. 2022). The steady state of SOC stocks theoretically represents the long-term balance between NPP and soil respiration. However, the time required to reach a new steady state from a perturbed state, such as a land use change, varies greatly from warm to cold regions (Smith 2005). On a global scale, the IPCC guidelines for greenhouse gas inventories recommend a minimum of 20 years for SOC to approach a new steady state (Eggleston et al. 2006). Therefore, resolving the steady-state relationship between different climates and SOC is key to reducing uncertainty in climate-carbon cycle feedbacks.

SOC models typically define various carbon pools based on turnover time and predict future SOC stocks by calculating the input and output fluxes of different carbon pools in response to climate change (Wang et al. 2013; Wieder et al. 2014; Ahrens et al. 2015; Abramoff et al. 2022). However, the performance of those models can be impaired not only by uncertainty of model structure and parameters, but also by limited data availability (Shi et al. 2018; Wieder et al. 2018). Also, the uncertainty rises as the spatial scale increases (Wiesmeier et al. 2019). Therefore, many efforts have been made to delineate soil zones and estimate soil organic matter by constructing climate indices (Jenny 1980; Yi et al. 1996). Generally, the climate indices is composed of several multiplied equations, among which the temperature equation is usually in exponential form, and the water equation has multiple different forms of equations depending on the proxy (precipitation, soil moisture content, water potential, etc.) used (Qi and Ming 2001). However, the importance of different climate factors remains controversial (Giardina et al. 2014; Canarini et al. 2017; Fang et al. 2018), and no consensus on a global, intuitive and clear climate-SOC relationship has coalesced.

In recent years, extensive soil mapping data and machine learning developments have resulted in global SOC databases (Batjes et al. 2017; Hengl et al. 2017) that can help identify global climate-SOC relationships. Here, we constructed three climate indices to explore their performance as SOC predictors at different time scales and soil depths (Figure 1). We hypothesize that (1) relationships between climate and SOC are distinct at different soil depths and (2) climate indices would perform more stably over longer timescales and perform better in shallower soils because shallow soils are more responsive to climate and will therefore reach steady state over a shorter time period.

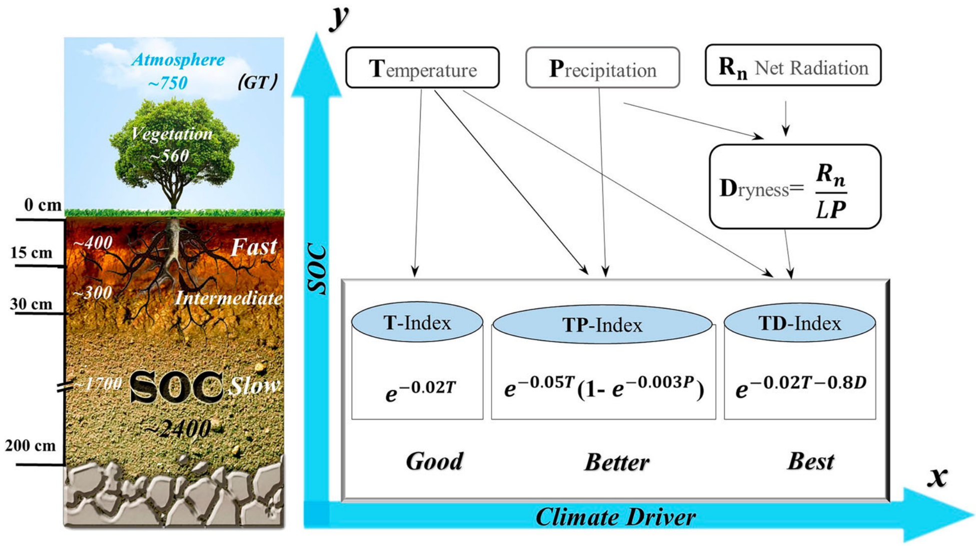

Figure 1. Climatic drivers of soil organic carbon (SOC) storage. The SOC data were retrieved from the International Soil Reference and Information Centre (ISRIC). Three climate indices, namely T-Index, P-Index, and TD-Index, were defined by Equations (3)–(5). The climate variables, including temperature (T), precipitation (P), and net radiation (R_n), represent the long-term annual mean values from 1916 to 2015. Temperature and precipitation data were sourced from the Climatic Research Unit (CRU) of the University of East Anglia (CRU TS v. 4.04), while net radiation data were calculated using National Oceanic and Atmospheric Administration (NOAA) data. All climate data were resampled to a 0.5°×0.5° grid resolution using nearest neighbour interpolation. Further details on why the TD-Index is identified as the best predictor can be found in Figure 2.

2. Methods

2.1. Climate data

Annual mean temperature and precipitation data spanning from 1916 to 2015 were obtained from the Climatic Research Unit (CRU) of the University of East Anglia (Harris et al. 2014). The climate data have a spatial resolution of 0.5 degrees latitude/longitude (CRU TS v. 4.04). Mean net radiation data for the same period were derived from monthly values provided by the National Oceanic and Atmospheric Administration (NOAA) reanalysis, with a resolution of one degree (Slivinski et al. 2019). To achieve a consistent resolution, a nearest neighbour interpolation approach was employed to downscale the one-degree resolution data to a 0.5-degree resolution. Net radiation was determined as the difference between net incoming shortwave radiation and net longwave radiation for each month, then aggregated to annual mean values. The dryness (D) was calculated by:

$$D = \frac{R_n}{\mathrm{LP}} \tag{1}$$

where R_n (MJ m^{-2} yr^{-1}) is mean annual net radiation, P (mm yr^{-1}) is mean annual precipitation, and L (= 2.5 MJ kg^{-1}) is the enthalpy of vapourization. The grids with no precipitation or negative net radiation were removed before final analysis.

2.2. SOC data

SOC data for six standard depth intervals were obtained from the International Soil Resource and Information Center (ISRIC) (Batjes et al. 2017). The ISRIC data has gained broad consensus and is widely used for studying SOC loss dynamics resulting from land-use practices (Sanderman et al. 2017). The original spatial resolution of the SOC database was 250 m, which was upscaled to a resolution of 0.5°×0.5° using nearest neighbour interpolation.

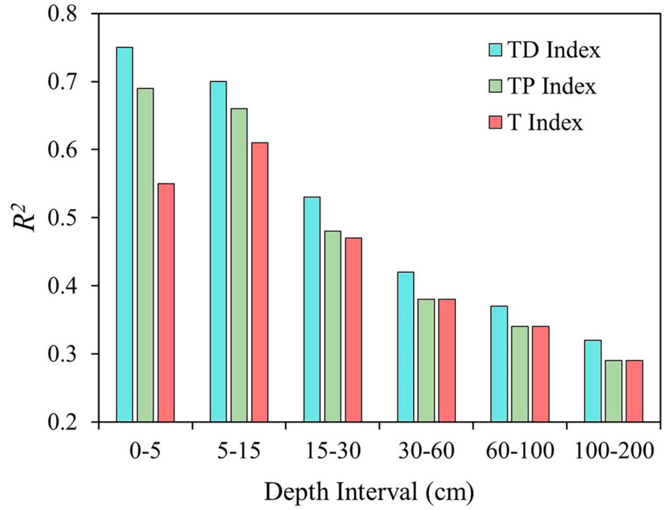

Figure 2. Performance summary of the Boltzmann-Sigmoidal Model (BSM) using three different climate indices for each of the six soil layers. The three indices, defined by Equations (2)–(4), are utilized in the BSM represented by Equation (6). The bars in the figure represent the amount of variance explained (R^2) by each predictor (index) in the respective soil layer. The p-value < 0.001 for each fit. Corresponding AICs can be seen in Extended Data Table A1.

2.3. Climate indices

An empirical model proposed by Jenny (1980) for modelling the synergistic control of temperature and precipitation on soil nitrogen concentration as:

$$\mathrm{N} = 55\, e^{-0.08T}(1 - e^{-0.005P/Q}) \tag{2}$$

where N is soil organic nitrogen content (%), T and P are long-term annual mean temperature (°C) and precipitation (mm yr^{-1}) respectively, and Q is vapour pressure deficit (k Pa).

Yi et al. (1996) modified Jenny's formula which successfully predicted Chinese soil types based on a 40-year average of observational temperature and precipitation.

Considering the coupling of the terrestrial carbon and nitrogen cycles and the similar response of soil carbon and nitrogen to different environments (Redfield 1958; Thornton and Rosenbloom 2005), we hypothesize that similar climatic indices may also be valid in predicting SOC. Through statistical correlation analysis, three climate indices were identified as performing better when considering either single or combinations of different climate factors: the T-Index, the TP-Index, and the TD-Index. The T-Index is defined as:

$$\text{T-Index} = e^{-0.02T} \tag{3}$$

where T is mean annual temperature (°C) at a grid cell. The TP-Index was defined as:

$$\text{TP-Index} = e^{-0.05T}(1 - e^{-0.003P}) \tag{4}$$

where P is mean annual precipitation (mm yr^{-1}) at a grid cell. the TD-Index as:

$$\text{TD-Index} = e^{-0.02T-0.8D} \tag{5}$$

where D is dryness defined by (1). Parameters in the indices were determined by fitting the highest coefficient of determination (R^2) and lowest root mean squared error (RMSE).

2.4. BSM

The relationship between SOC and climate variables usually exhibits sigmoidal behaviour, where the rate of SOC accumulation or depletion saturates with changing climatic conditions. We applied BSM, a modified logistic sigmoidal function by Boltzmann to fit the relationship of SOC and the climatic indices. BSM is written as:

$$y = A_2 + \frac{A_1 - A_2}{1 + e^{\frac{x - x_0}{dx}}} \tag{6}$$

where y represents SOC (t/ha), x represents one of three climatic indices, the parameters A_1 and A_2 are the magnitudes of SOC for $x \to 0$ and $x \to \infty$, respectively, x_0 is the inflection point and $dx$is the slope at the inflection point. We made the assumption that steady states of SOC stocks and climate can be approximated by their long-term means (Yi and Jackson 2021).

2.5. Model analysis for steady-state of SOC and temperature

The scatterplot SOC-TD-Index on 100-year scale of different soil layers were grouped by TD-Index with a 0.1 interval (see Extended Data Figure A3). The mean SOC and temperature values were averaged from different TD-Index groups. The linear model was first used to fit the steady state of SOC and temperature. We observed that in the steady-state relationship between SOC and temperature, there appears to be a temperature breakpoint. Below this breakpoint, SOC changes minimally, while above it, SOC decreases almost linearly with temperature. To detect the presence of this temperature breakpoint, we referred to the approach in Johnston and Sibly (2018) to compare the linear model with a threshold model, which is defined as follows:

$$\mathrm{SOC} = \begin{cases} C, & T \leq T_0 \\ a(T - T_0) + C, & T > T_0 \end{cases} \tag{7}$$

where C is a constant SOC value, T_0 is the temperature breakpoint, a is slope of the linear decreasing phase.

Temperature breakpoints were examined within the temperature range of 17.4–22.4°C, with increments of 0.1°C. Subsequently, differences in AICs (Akaike Information Criteria) of the linear and threshold models were compared for each temperature breakpoint. The temperature breakpoint resulting in the greatest ΔAIC was considered to be the one with the strongest endorsement, provided that ΔAIC exceeded 5 for extra degrees of freedom and $P < 0.05$ in a likelihood ratio test.

3. Results

We utilized the BSM represented by Equation (6) to assess the performance of the three indices.

Initially, we applied these indices to six soil depth intervals (Figure 2). While various factors contribute to the balance of SOC stocks, temperature emerges as a dominant factor, and thus, the T-Index significantly explains the variability in SOC stocks. The TP-Index performs better than the T-Index since it incorporates the effect of precipitation (as shown in Figure 2). Despite the better performance of the TP-Index, it does not consider the processes of light control on organic matter inputs to SOC stocks through photosynthesis or the contribution of evapotranspiration to the soil water balance. In contrast, the dryness index (D) provides a more comprehensive characterization of the energy and water balance. Our results demonstrate that the TD-Index outperforms the other two indices in capturing variations in SOC stocks (as illustrated in Figure 2), as summarized in Figure 1.

Our findings indicate that the TP-Index does not significantly differ from the T-Index in its ability to explain variations in SOC stocks in deeper soil layers (as shown in Figure 2). This suggests that the influence of precipitation on SOC stocks differs between the top soil and deep soil. On a global scale, more than half of the SOC is stored below 20 cm, but precipitation plays a lesser role in deep soil compared to the topsoil (Engelhardt et al. 2018). As the soil gets deeper, each of the three climate indices explains a smaller percentage of the variation in SOC. This implies that climate has less influence on SOC the deeper the soil layer is on the timescales in this study.

To assess the sensitivity of the BSM parameters to different time scales, we conducted sensitivity tests using the SOC data spanning a 100-year period from 1916 to 2015. Initially, we divided this 100-year period into 10 ten-year intervals, resulting in 10 sets of BSM parameters for each SOC pool (as shown in Figure 2). Subsequently, we estimated the values of the four BSM model parameters or nine twenty-year groups by shifting the time window by 10 years (as illustrated in Extended Data Figure A1). By doing so, we obtained the values of the four BSM model parameters for 55 groups representing different time scales, ranging from 10 years to 100 years (as depicted in Extended Data Figure A2). This analysis revealed that the values of the BSM model parameters for different time scales tend to converge rather than diverge. Outliers were primarily observed on the ten-year and twenty-year time scales, with fewer outliers on the twenty-year time scale compared to the ten-year time scale (as presented in Extended Data Table A2). Based on these findings, we conclude that the BSM model parameters exhibit insensitivity to the length of the time period when the time scale is longer than 20 years.

Given the best performance of TD-Index and the validity of the steady-state assumption, the BSM with TD-Index on 100-year scale is used in the following analysis. Due to the similar performance of the indices at certain soil depths, we merged the depth intervals into three categories: a top layer from 0 to 15 cm, a transitional layer from 15 to 30 cm, and a deep layer from 30 to 200 cm (as depicted in Figure 3). As expected, Figure 3 confirms that the impact of climate on SOC stocks decreases significantly with soil depth. The TD-Index is able to explain 74% of the variation in SOC stocks in the top soil layer (0–15 cm), but only 35% in the deep soil layer (30–200 cm) and 53% in the transitional layer (15–30 cm). An increase in temperature or a decrease in the aridity index leads to an increase in the TD-Index, so an increase in the TD-Index indicates better hydrothermal conditions for SOC sequestration. TD-Index shows the same spatial heterogeneity as the soil organic carbon, especially in fast pool, with a correspondingly high stock of soil organic carbon where the TD-Index is high (Extended data Figure A4).

The BSM pattern of SOC and TD-Index can be broadly divided into three phases. With an increase in TD-Index, SOC shows a gradual rise initially, followed by a rapid ascent, and ultimately stabilizes. This suggests the potential presence of climatic tipping points for SOC. Especially the transition from a high-stability phase to a rapid-change phase may signify substantial losses in SOC. In this regard, we transformed the scatter data from Figure 3 into boxplot distributions, as shown in Extended Data Figure A3. From these mean values in the noise-free boxplot, we first conducted an analysis of the steady-state of SOC and temperature by comparing the linear and threshold models (see Method). The results indicate that the temperature breakpoints for the SOC-temperature relationship, ranging from the upper soil layer to the deeper soil layers, are −4.3, −4.5, and −3.0°C, respectively (Figure 4). When the temperature falls below the breakpoints, SOC remains high and varies minimally with temperature changes. Conversely, when the temperature surpasses the breakpoints, SOC experiences a rapid decline. This phenomenon is particularly pronounced in the top and transition soil layers. In the deeper soil fluctuations around an MCT of approximately 20°C across soil layers, we did not detect breakpoints in these cases. In terms of the steady state of SOC and dryness, we observed a consistent pattern across different soil layers. SOC levels were notably high in wet conditions, while a distinct decrease was observed near a dryness index of 1 (Figure 4).

4. Discussion and conclusions

We consolidate multiple climate factors influencing SOC stocks into a single TD-Index, representing a century-scale steady-state framework. Our study demonstrates stable climate indices'

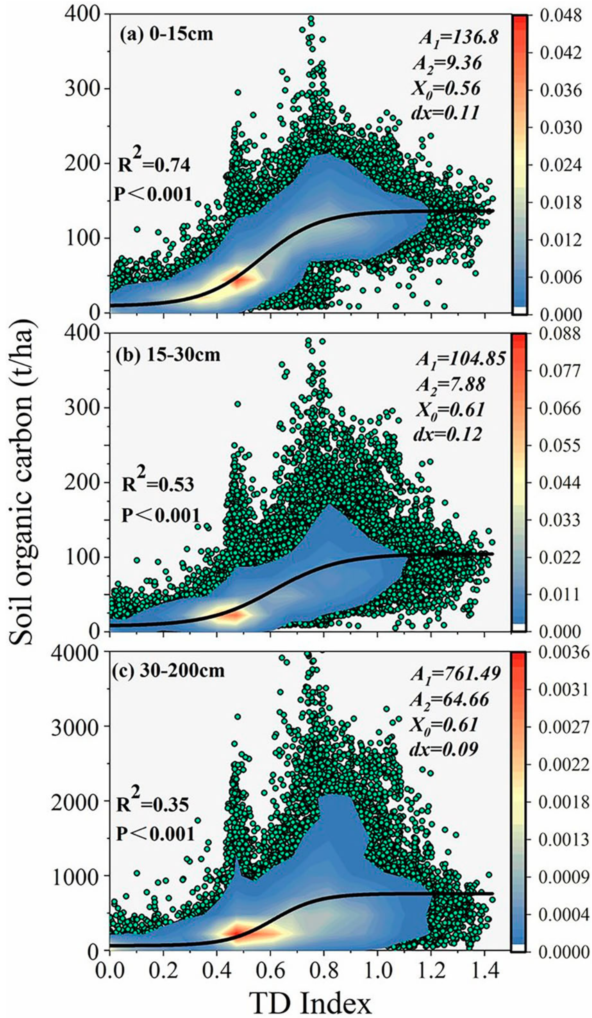

Figure 3. TD-Index as a predictor of soil organic carbon (SOC) in three soil layers: (a) Fast carbon pool (0–15 cm); (b) Transitional carbon pool (15–30 cm); and (c) Slow carbon pool (30–200 cm). The scatter data points of SOC vs TD-Index, with a resolution of 0.5°×0.5°, are represented by filled blue circles. Grid cells with missing data or negative net radiation (*Rn*) values were excluded from the analysis. The colour clouds depict the overall density distribution of the data points, smoothed using a nonparametric Kernel density technique. The black lines correspond to the fitting curves obtained from the Boltzmann-Sigmoidal Model (BSM) (6) using the SOC and TD-Index data, and the values of the four model parameters are provided for each soil layer. Further details on the BSM can be found in the Methods section.

performance over longer scales and in shallower soils. The TD-Index outperformed the TP-Index or temperature alone because dryness, as defined by Budyko (1961), encompasses not only the effect of precipitation but also the influence of net radiation. This comprehensive index provides a better understanding of the fundamental nature of dryness and its impact on SOC stocks. Consistent with previous studies, our results suggest that SOC stock is higher in cold and humid places, while lower in hot and dry regions (Post et al. 1982; Jobbágy and Jackson 2000; Crowther et al. 2019). Importantly, this indicates the regulation of warming-induced carbon loss by drought. Water stress limits photosynthesis reducing organic carbon input, but at the same time soil respiration is weakened due to reduced microbial activity and availability of substrates for decomposition (Davidson and Janssens 2006; Davidson 2020). Wetlands and cold regions exhibit the highest accumulation of carbon stocks, indicating that cold or waterlogged conditions have a greater impact on reducing respiratory

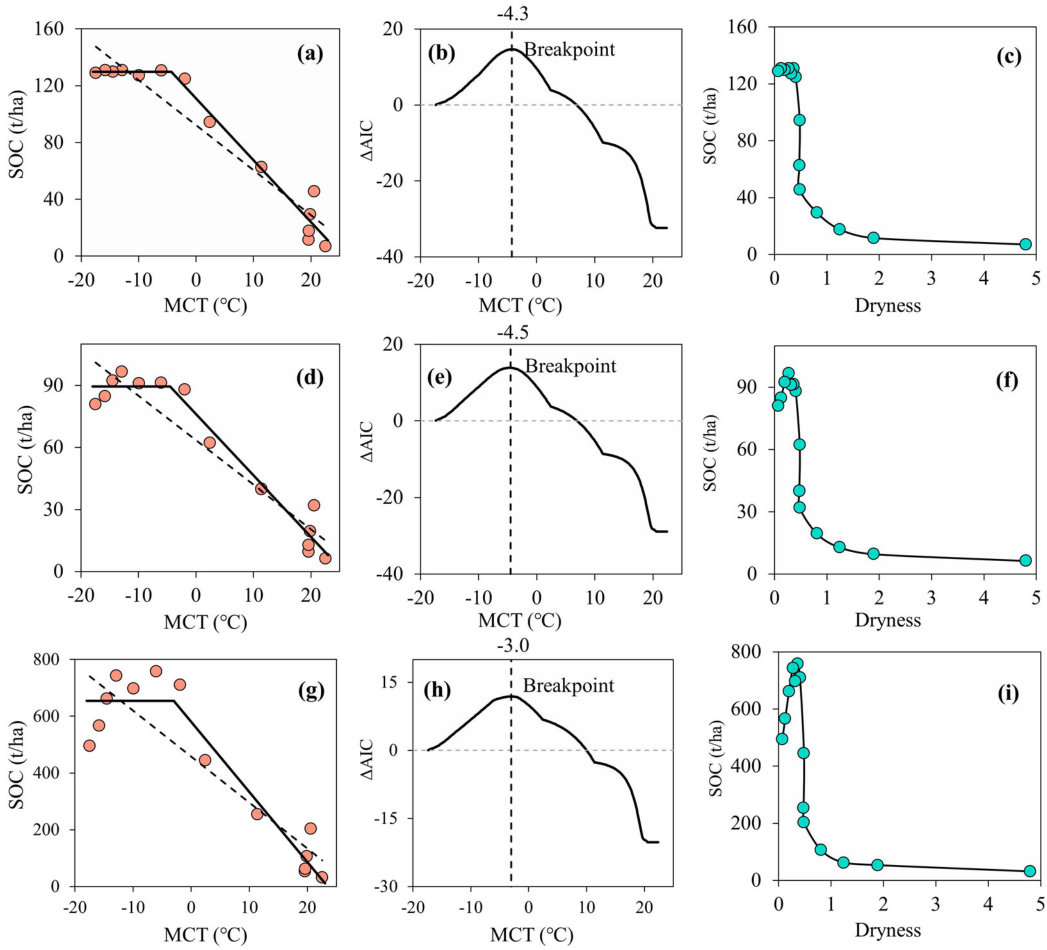

Figure 4. Steady state of soil organic carbon (SOC)- temperature and SOC-dryness. The mean SOC and mean century temperature (MCT) values presented in panels (a) top pool (0–15 cm), (d) transitional pool (15–30 cm), and (g) deep pool were derived from the scatter data in Figure 2, grouped by TD-Index with a 0.1 interval (see Extended Data Figure A3). The dashed and solid lines represent the prediction from the linear and threshold models (see Method) of the SOC-temperature steady state, respectively, with R_L^2 and R_T^2 goodness of fit. (b), (e) and (h) show the temperature breakpoints for top to deep soil layers, identified by the difference in AIC (Akaike Information Criteria) of threshold to linear model where higher values provide a better fit. (c), (f) and (i) present steady state of SOC-dryness, derived the same way as we obtained the SOC-MCT relationship.

carbon losses compared to primary production (Crowther et al. 2019). Besides, the imbalance is also related to vegetation types and biomass abundance (Wang et al. 2003; Frank et al. 2012; Canarini et al. 2017). Temperature sensitivity (Q_{10}) of SOC decomposition varies widely among vegetation types. The composition of soil bacteria and C:N concentrations which structured primarily by vegetation types, driving fundamentally different response of SOC dynamic to climate change (Bates et al. 2018).

Our results support previous isotopic SOC studies (Balesdent et al. 2018), which have shown that SOC responses to climate exhibit layering effects, with different responses observed in the topsoil compared to the deep soil. In the topsoil layer, the evolution of SOC stocks is driven by the balance between net primary production (NPP) and soil respiration, which is influenced by climate factors through intricate feedback connections (Heimann and Reichstein 2008). For instance, autotrophic processes associated with NPP are closely linked to heterotrophic soil microorganisms involved in respiration. However, autotrophic processes are often limited by nitrogen availability, while

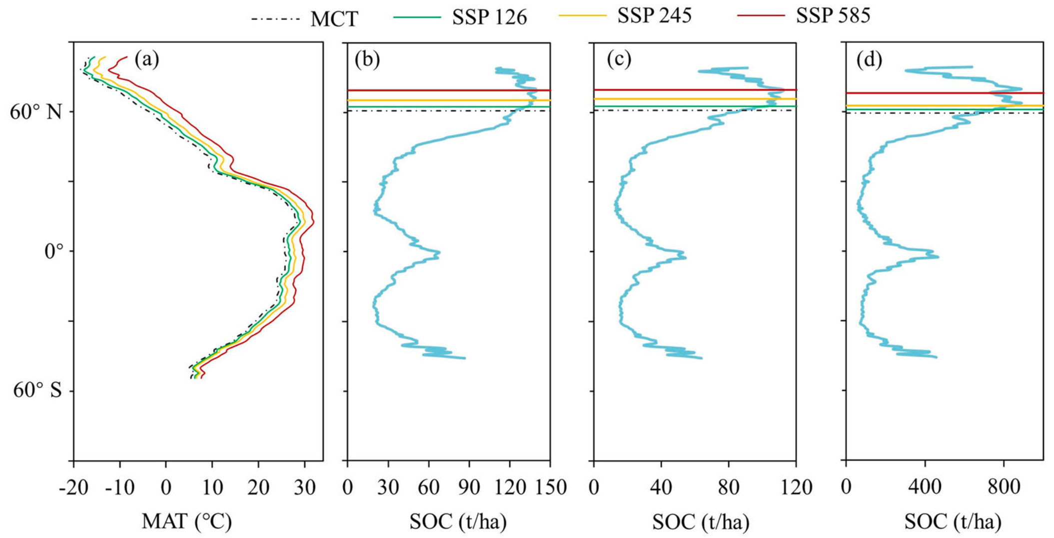

Figure 5. The latitudinal shift of breakpoint temperature for different soil layers. (a) The latitudinal mean century temperature (MCT) and the prediction of the latitudinal mean annual temperature with three emission scenarios by the end of twenty-first century (2080–2100) based on BCC-CMS2-MR model from CMIP 6. The breakpoint temperatures are −4.3°C, −4.5°C and −3.0°C for top, transitional and deep soil layer, whose latitudinal shift prediction with different emission scenarios are shown on (b), (c) and (d) respectively. The blue curve represents the latitudinal mean SOC of different soil layers.

heterotrophic communities and activities are limited by labile soil carbon (Tiessen et al. 1994). Both autotrophic and heterotrophic processes co-vary with climate, but they follow different pathways (Crowther et al. 2019). The feedback loops and response patterns in the topsoil layer are complex due to these interconnections (Balesdent et al. 2018).

As we move deeper into the soil profile, the abundance of bacteria, fungi, plant inputs, rhizosphere, and variability in soil moisture diminish. Soil carbon in deeper layers tends to be older, and the biotic communities are more persistent (Soong et al. 2020). The carbon inputs from plants and their roots, which fuel the metabolism of heterotrophic soil microorganisms, remain concentrated in the topsoil layers and exhibit stronger feedback with precipitation. In contrast, the microbial communities in the deeper soil layers are less abundant, older, and more resilient to water conditions. Moreover, precipitation (P) represents only the input component of the soil water budget, while the output component is primarily driven by evapotranspiration, which is influenced by temperature (T) and net radiation (R_n). The Budyko dryness index (D) combines both the energy and water balance components and is closely linked to productivity. Therefore, it is conceptually reasonable that the TD-Index, which incorporates both temperature and dryness, demonstrates a greater ability to explain the climate controls on SOC stocks from the top to the bottom soil layers, compared to other climate indices (Figure 1). Additionally, labile carbon becomes extremely limited in deep soils (Rumpel and Kögel-Knabner 2011; Balesdent et al. 2018). Microorganisms in deep soil are adapted to environmental conditions with less climate variability and higher limitations in labile carbon availability. As a result, they become more resistant and resilient to changes (Yi and Jackson 2021). Consequently, deep SOC stocks are less affected by climate compared to shallow ones (Mathieu et al. 2015). Not only that, but deeper SOC are also less susceptible to land use land cover change. Studies have shown that carbon loss due to land use change decreases exponentially with soil depth (Guo and Gifford 2002).

The identification of the SOC-temperature century-steady-state presents both new opportunities and challenges for SOC dynamic modelling. It highlights the need for long-term data collection to capture the dynamics and shifts in SOC stocks under changing climate conditions. Moreover, it

Table 1. The latitude of breakpoint for different soil layers for last century and their prediction for the end of the twenty-first century (2080–2100) under different emission scenarios based on the BCC-CMS2-MR model and the corresponding increased vulnerable area for soil organic carbon loss.

	Latitude of breakpoint (°N)				Increased vulnerable area (10^6 km^2)		
Soil layers	Historical	SSP 126	SSP 245	SSP 585	SSP 126	SSP 245	SSP 585
Top	60.7	62.5	65.3	69.5	3.6	8.3	12.4
Transitional	60.9	62.7	65.8	69.8	3.5	8.5	12.5
Deep	59.4	60.9	62.7	68.1	2.1	5.6	12.2

emphasizes the importance of focusing on the breakpoint temperatures and their potential shifts in response to ongoing climate warming. For example, we analysed the latitudinal shift of breakpoint temperature by the end of twenty-first century (2080–2100) for different soil layers with three emission scenarios based on BCC-CMS2-MR model (Xin et al. 2013). We can see that under the low emissions scenario, the latitudinal breakpoint line moves very little northwards, whereas in the high emissions scenario, sizable northern regions with large SOC stocks will warm up above the breakpoint. (Figure 5, Table 1).

Vulnerable to climate change, SOC may reach a tipping point, releasing massive CO2 into the atmosphere. Although the temperature breakpoints in this study are not climate tipping points, especially for deep soils where the SOC response to climate is insensitive and slow, they are reminders of the importance of carbon loss from warming in soil management. The hot areas of land are likely to experience enhancement (Yi et al. 2014), and the warming is expected to have Arctic amplification (Serreze and Barry 2011). Understanding these shifts and their implications is crucial for effectively managing soil carbon stocks in a future with a global climate warmer by 1.5°C or more.

Taken together, our findings provide valuable insights and open up new avenues for research and management strategies related to SOC dynamics. By considering the TD-Index and its implications, future studies can advance our understanding of climate controls on SOC stocks. It could be used to identify likely future hotspots of SOC loss which could guide experimental measurements, refine SOC modelling approaches, and inform water resource planning strategies for sustainable soil management in different climatic regimes.

Acknowledgements

CY completed this research when he was a Fulbright Visiting Professor at University of Innsbruck with support from the US-Austria Fulbright Program. DC is supported by the Swedish national strategic research area BECC and Swedish Research Council (VR: 2021–02163 and 2022-06011).

Disclosure statement

No potential conflict of interest was reported by the author(s).

Notes on contributors

Qin Zhang is a PhD student at the Dalian University of Technology, Dalian, China. His main research interest is the regulation of water on climate-carbon cycle feedback mechanism.

Dr. Chuixiang Yi is a professor of Queens College of City University of New York, New York, USA. His research is focused on canopy fluid mechanics including developing theoretical formulations, designing observations, and performing numerical simulations to understand the physical, biological, and chemical processes that control the exchange of trace gas between the vegetation and the atmosphere. Yi was a leading recipient of World Meteorological Organization Norbert-Gerbier-MUMM International Award in 2012. Yi was a Rossby Fellow from International Meteorological Institute at Stockholm University during 2014–2015 and a Fulbright Visiting Professor at University of Innsbruck in 2022–2023. His Lab has a broad spectrum of research projects across Forest Ecology, Remote Sensing, Micrometeorology, Climate Change, Paleoclimate, and Hydrology. The overall goal of his team is to use nonlinear system theory, stability analysis approach, resilience, and tipping point concepts to predict potential critical transitions of nature and society in facing extremes induced by the warming climate.

Dr. Georg Wohlfahrt is an associate professor of ecology at the Universität Innsbruck Innsbruck, Austria. He has a general interest in biosphere-atmosphere interactions and feedbacks with a focus on improving carbon cycle estimates, especially of gross primary productivity and ecosystem respiration.

Dr. Deliang Chen is a professor of Physical Meteorology and August Röhss Chair in Physical Geography at the University of Gothenburg, Gothenburg, Sweden. His main research interests are Earth System Science and global environmental change with a focus on climate change and impacts in Europe and Asia. He is an elected member of seven Academies in the world including the Royal Swedish Academy of Sciences and The World Academy of Sciences. He has served on numerous international and national committees and boards, as well as advised various governmental, intergovernmental, and international non-governmental bodies including funding agencies. A recent example is his role in the 6th IPCC Working Group I assessment report as a coordinating lead author.

Dr. *Max Rietkerk* is **a** professor of Spatial Ecology and Global Change at Utrecht University, TC Utrecht, the Netherlands. His research and teaching is about Ecology, Environmental Sciences, and current topics on Global Change and Ecosystems. His research concentrates on Spatial Ecology and Global Change. His research has been published in more than 100 articles in international refereed scientific journals, including top journals such as Nature and Science.

Dr. Zhenkun Tian is an associate professor of Mathematics and Computer of China University of Labor Relations, Beijing, China. His main research interests are climate-carbon cycle related digital image processing, remote sensing applications, machine learning, spatial data analysis.

Dr. Mousong Wu is an associate professor of Earth System Science of Nanjing University, Nanjing, China. His main research interests are terrestrial carbon cycle and data assimilation; algorithms for assimilating data from multi-source remote sensing observations; hydrological and ecosystem processes in cold regions; development and application of coupled soil-plant-atmosphere water-heat-carbon and nitrogen models; water-carbon management in agriculture under changing climate conditions.

Dr. Eric Kutter is a researcher of Barry Commoner Center for Health & the Environment, Queens College, City University of New York, Flushing, USA. His main research interests are fluxes of CO_2, H_2O and energy in forest ecosystems using towers for eddy-covariance and vertical profile measurements; improving measurement methods and analyzing measurement data.

Jianxu Han is a PhD student at the Dalian University of Technology, Dalian, China. Her main research interest is water environment pollution management and watershed Modelling.

Dr. George Hendrey is a retired Distinguished Professor in the School of Earth and Environmental Science of Queens College, City University of New York, New York, USA. He is the designer for Free-Air CO2 Enrichment (FACE) experiments, testing global ecosystem responses to future increases in atmospheric CO2. He has been working on development of a NPP correction based on photosynthesis experiments in which CO2 is oscillated in a controlled way in a leaf chamber while measuring photosynthetic fluorescence and/or CO2 assimilation.

Dr. Shiguo Xu is a professor of hydrology of Dalian University of Technology, Dalian, China. His main research interests are rainwater resource utilization and management; Environmental water resources system analysis; Wetland water cycle and ecological environment management; Environmental protection and construction of rivers and watersheds; Reservoir pollution prevention and management.

Data availability statement

Long-term temperature and precipitation derived from CRU TS v. 4.04 are publicly available at https://crudata.uea.ac.uk/cru/data/hrg/cru_ts_4.04/. Long-term radiation data are publicly available at https://psl.noaa.gov/data/gridded/data.20thC_ReanV3.html. SOC data are publicly available at https://data.isric.org/geonetwork/srv/chi/catalog.search#/metadata/98062ae9-911d-4e04-80a9-e4b480f87799. The CMIP6 data are publicly available at https://esgf-node.llnl.gov/projects/cmip6/. All other data that support the plots within this paper and other findings of this study are available from the corresponding author upon reasonable request.

References

Abramoff RZ, Guenet B, Zhang H, Georgiou K, Xu X, Rossel RAV, Yuan W, Ciais P. 2022. Improved global-scale predictions of soil carbon stocks with Millennial Version 2. Soil Biol Biochem. 164:108466. doi:10.1016/j.soilbio.2021.108466.

Ahrens B, Braakhekke MC, Guggenberger G, Schrumpf M, Reichstein M. 2015. Contribution of sorption, DOC transport and microbial interactions to the 14C age of a soil organic carbon profile: insights from a calibrated process model. Soil Biol Biochem. 88:390–402. doi:10.1016/j.soilbio.2015.06.008.
Balesdent J, Basile-Doelsch I, Chadoeuf J, Cornu S, Derrien D, Fekiacova Z, Hatté C. 2018. Atmosphere–soil carbon transfer as a function of soil depth. Nature. 559:599–602. doi:10.1038/s41586-018-0328-3.
Bates ST, Clemente JC, Flores GE, Walters WA, Parfrey LW, Knight R, Fierer N, . 2018. Global biogeography of highly diverse protistan communities in soil. ISME J. 7(3):652–659. doi:10.1038/ismej.2012.147.
Batjes NH, Ribeiro E, Oostrum AV, Leenaars J, Hengl T, Jesus JM. 2017. WoSIS: providing standardised soil profile data for the world. Earth Syst Sci Data. 9:1–14. doi:10.5194/essd-9-1-2017.
Budyko MI. 1961. The heat balance of the earth's surface. Sov Geogr. 2:3–13.
Canarini A, Kiær LP, Dijkstra FA. 2017. Soil carbon loss regulated by drought intensity and available substrate: A meta-analysis. Soil Biol Biochem. 112:90–99. doi:10.1016/j.soilbio.2017.04.020.
Clarke J, Huntingford C, Ritchie P, Cox P. 2021. The compost bomb instability in the continuum limit. Eur. Phys. J. Spec. Top. 230:3335–3341. doi:10.1140/epjs/s11734-021-00013-3.
Cox PM, Betts RA, Jones CD, Spall SA, Totterdell IJ. 2000. Acceleration of global warming due to carbon-cycle feedbacks in a coupled climate model. Nature. 408:184–187. doi:10.1038/35041539.
Crowther TW, Hoogen JV, Wan J, Mayes MA, Keiser AD, Mo L, Averill C, Maynard DS. 2019. The global soil community and its influence on biogeochemistry. Science. 365:eaav0550. doi:10.1126/science.aav0550.
Davidson EA. 2020. Carbon dioxide loss from tropical soils increases on warming. London: Nature Publishing Group UK.
Davidson EA, Janssens IA. 2006. Temperature sensitivity of soil carbon decomposition and feedbacks to climate change. Nature. 440:165–173. doi:10.1038/nature04514.
Doetterl S, Stevens A, Six J, Merckx R, Oost K, Pinto MC, Casanova-Katny A, Muñoz C, Boudin M, Venegas EZ. 2015. Soil carbon storage controlled by interactions between geochemistry and climate. Nat Geosci. 8:780–783. doi:10.1038/ngeo2516.
Eggleston HS, Buendia L, Miwa K, Ngara T, Tanabe K. 2006. IPCC guidelines for national greenhouse gas inventories. https://www.ipcc-nggip.iges.or.jp/public/2006gl/index.html
Engelhardt IC, Welty A, Blazewicz SJ, Bru D, Rouard N, Breuil MC, Gessler A, Galiano L, Miranda JC, Spor A. 2018. Depth matters: effects of precipitation regime on soil microbial activity upon rewetting of a plant-soil system. ISME J. 12:1061–1071. doi:10.1038/s41396-018-0079-z.
Fang Q, Wang G, Xue B, Liu T, Kiem A. 2018. How and to what extent does precipitation on multi-temporal scales and soil moisture at different depths determine carbon flux responses in a water-limited grassland ecosystem? Sci Total Environ. 635:1255–1266. doi:10.1016/j.scitotenv.2018.04.225.
Frank DA, Pontes AW, McFarlane KJ. 2012. Controls on soil organic carbon stocks and turnover among North American ecosystems. Ecosystems. 15:604–615. doi:10.1007/s10021-012-9534-2.
Friedlingstein P, Cox P, Betts R, Bopp L, Bloh W, Brovkin V, Cadule P, Doney S, Eby M, Fung I. 2006. Climate–carbon cycle feedback analysis: results from the C4MIP model intercomparison. J Clim. 19:3337–3353. doi:10.1175/JCLI3800.1.
Giardina CP, Litton CM, Crow SE, Asner GP. 2014. Warming-related increases in soil CO2 efflux are explained by increased below-ground carbon flux. Nat Clim Change. 4:822–827. doi:10.1038/nclimate2322.
Guo LB, Gifford R. 2002. Soil carbon stocks and land use change: A meta analysis. Glob Change Biol. 8:345–360. doi:10.1046/j.1354-1013.2002.00486.x.
Harris I, Jones PD, Osborn TJ, Lister DH. 2014. Updated high-resolution grids of monthly climatic observations–the CRU TS3. 10 Dataset. Int J Climatol. 34:623–642. doi:10.1002/joc.3711.
Hartley IP, Hill TC, Chadburn SE, Hugelius G. 2021. Temperature effects on carbon storage are controlled by soil stabilisation capacities. Nat Commun. 12:6713. doi:10.1038/s41467-021-27101-1.
Heimann M, Reichstein M. 2008. Terrestrial ecosystem carbon dynamics and climate feedbacks. Nature. 451:289–292. doi:10.1038/nature06591.
Hengl T, Jesus JM, Heuvelink GBM, Gonzalez MR, Kilibarda M, Blagotić A, Wei S, Wright MN, Geng X, Bauer-Marschallinger B. 2017. Soilgrids250m: global gridded soil information based on machine learning. PLoS One. 12:e0169748. doi:10.1371/journal.pone.0169748.
Jenny H. 1980. The soil resource: origin and behavior. New York: Springer.
Jobbágy EG, Jackson RB. 2000. The vertical distribution of soil organic carbon and its relation to climate and vegetation. Ecol Appl. 10:423–436. doi:10.1890/1051-0761(2000)010[0423:TVDOSO]2.0.CO;2.
Johnston ASA, Sibly RM. 2018. The influence of soil communities on the temperature sensitivity of soil respiration. Nat Ecol Evol. 2:1597–1602. doi:10.1038/s41559-018-0648-6.
Koven CD, Hugelius G, Lawrence DM, Wieder WR. 2017. Higher climatological temperature sensitivity of soil carbon in cold than warm climates. Nat Clim Change. 7:817–822. doi:10.1038/nclimate3421.
Luo Z, Feng W, Luo Y, Baldock J, Wang E. 2017. Soil organic carbon dynamics jointly controlled by climate, carbon inputs, soil properties and soil carbon fractions. Glob Chang Biol. 23:4430–4439. doi:10.1111/gcb.13767.

Mathieu JA, Hatté C, Balesdent J, Parent E. 2015. Deep soil carbon dynamics are driven more by soil type than by climate: a worldwide meta-analysis of radiocarbon profiles. Glob Chang Biol. 21:4278–4292. doi:10.1111/gcb.13012.

Melillo JM, Frey SD, DeAngelis KM, Werner WJ, Bernard MJ, Bowles FP, Pold G, Knorr MA, Grandy AS. 2017. Long-term pattern and magnitude of soil carbon feedback to the climate system in a warming world. Science. 358:101–105. doi:10.1126/science.aan2874.

Nottingham AT, Meir P, Velasquez E, Turner BL. 2020. Soil carbon loss by experimental warming in a tropical forest. Nature. 584:234–237. doi:10.1038/s41586-020-2566-4.

Post WM, Emanuel WR, Zinke PJ, Stangenberger AG. 1982. Soil carbon pools and world life zones. Nature. 298:156–159. doi:10.1038/298156a0.

Qi Y, Ming X. 2001. Separating the effects of moisture and temperature on soil CO2 efflux in a coniferous forest in the Sierra Nevada mountains. Plant Soil. 237:15–23. doi:10.1023/A:1013368800287.

Redfield AC. 1958. The biological control of chemical factors in the environment. Am Sci. 46:230A-21.

Rumpel C, Kögel-Knabner I. 2011. Deep soil organic matter—A key but poorly understood component of terrestrial C cycle. Plant Soil. 338:143–158. doi:10.1007/s11104-010-0391-5.

Sanderman J, Hengl T, Fiske GJ. 2017. Soil carbon debt of 12,000 years of human land use. PNAS. 114:9575–9580. doi:10.1073/pnas.1706103114.

Serreze MC, Barry RG. 2011. Processes and impacts of Arctic amplification: A research synthesis. Glob Planet Change. 77:85–96. doi:10.1016/j.gloplacha.2011.03.004.

Shi Z, Crowell S, Luo Y, Moore B. 2018. Model structures amplify uncertainty in predicted soil carbon responses to climate change. Nat Commun. 9: 2171. doi:10.1038/s41467-018-04526-9.

Slivinski LC, Compo GP, Whitaker JS, Sardeshmukh PD, Giese BS, McColl C, Allan B, Yin X, Vose R, Titchner H. 2019. Towards a more reliable historical reanalysis: improvements for version 3 of the twentieth century reanalysis system. Quart J Roy Meteor Soc. 145:2876–2908. doi:10.1002/qj.3598.

Smith P. 2005. An overview of the permanence of soil organic carbon stocks: influence of direct human-induced, indirect and natural effects. Eur J Soil Sci. 56:673–680. doi:10.1111/j.1365-2389.2005.00708.x.

Soong JL, Phillips CL, Ledna C, Koven CD, Torn MS. 2020. CMIP5 models predict rapid and deep soil warming over the 21st century. J Geophys Res Biogeosci. 125:e2019JG005266. doi:10.1029/2019JG005266.

Thornton PE, Rosenbloom NA. 2005. Ecosystem model spin-up: estimating steady state conditions in a coupled terrestrial carbon and nitrogen cycle model. Ecol Modell. 189:25–48. doi:10.1016/j.ecolmodel.2005.04.008.

Tiessen H, Cuevas E, Chacon P. 1994. The role of soil organic matter in sustaining soil fertility. Nature. 371:783–785. doi:10.1038/371783a0.

Varney RM, Sarah EC, Friedlingstein P, Eleanor JB, Charles DK, Hugelius G, Cox PM. 2020. A spatial emergent constraint on the sensitivity of soil carbon turnover to global warming. Nat Commun. 11:5544. doi:10.1038/s41467-020-19208-8.

Wang G, Wilfred MP, Melanie AM. 2013. Development of microbial-enzyme-mediated decomposition model parameters through steady-state and dynamic analyses. Ecol Appl. 23:255–272. doi:10.1890/12-0681.1.

Wang W, Dalal RC, Moody PW, Smith CJ. 2003. Relationships of soil respiration to microbial biomass, substrate availability and clay content. Soil Biol Biochem. 35:273–284. doi:10.1016/S0038-0717(02)00274-2.

Wieder WR, Grandy AS, Kallenbach CM, Bonan GB. 2014. Integrating microbial physiology and physio-chemical principles in soils with the MIcrobial-MIneral Carbon Stabilization (MIMICS) model. Biogeosciences. 11:3899–3917. doi:10.5194/bg-11-3899-2014.

Wieder WR, Melannie DH, Benjamin NS, Wang Y, Dk C, Gordon BB. 2018. Carbon cycle confidence and uncertainty: exploring variation among soil biogeochemical models. Glob Chang Biol. 24:1563–1579. doi:10.1111/gcb.13979.

Wiesmeier M, Livia U, Eleanor UH, Birgit L, Margit L, Erika MS, Bas W, Eva R, Mareike L, Noelia GF. 2019. Soil organic carbon storage as a key function of soils - a review of drivers and indicators at various scales. Geoderma. 333:149–162. doi:10.1016/j.geoderma.2018.07.026.

Xin X, Wu T, Li J, Wang Z, Li W, Wu F. 2013. How well does BCC_CSM1. 1 reproduce the 20th century climate change over China? Atmos Oceanic Sci Lett. 6:21–26. doi:10.1080/16742834.2013.11447053.

Yi C, et al. 2010. Climate control of terrestrial carbon exchange across biomes and continents. Environ Res Lett. 5 (3):034007. doi:10.1088/1748-9326/5/3/034007.

Yi C, Jackson N. 2021. A review of measuring ecosystem resilience to disturbance. Environ Res Lett. 16: 053008. doi:10.1088/1748-9326/abdf09.

Yi C, Liu K, Li T. 1996. Research on relations of soil zonal distributions with climate in the monsoon region of the eastern part of China. Acta Pedol Sin. 33:390–396.

Yi C, Wei S, Hendrey G. 2014. Warming climate extends dryness-controlled areas of terrestrial carbon sequestration. Sci Rep. 4:5472. doi:10.1038/srep05472.

Appendix

Extended data

Extended data Table A1. AICs of the Boltzmann-Sigmoidal Model (BSM) using three different climate indices for each of the six soil layers.

	Soil layers					
Climate indices	0–5 cm	5–15 cm	15–30 cm	30–50 cm	50–100 cm	100–200 cm
TD Index	4.10×10^5	4.84×10^5	5.41×10^5	6.25×10^5	6.57×10^5	7.57×10^5
TP Index	4.23×10^5	4.99×10^5	5.48×10^5	6.28×10^5	6.61×10^5	7.61×10^5
T-Index	4.41×10^5	5.02×10^5	5.50×10^5	6.31×10^5	6.83×10^5	7.560×10^5

Extended data Table A2. Soil organic carbon (SOC) predictions of the Boltzmann-Sigmoidal Model (BSM) using different time periods.

		A1			A2			X0			dx		
Period		Fast	Transitional	Slow	Fast	Transitional	Slow	Fast	Transitional	Slow	Fast	Transitional	Slow
10 years	1	**136.2**	104	**753.3**	**9.63**	8.14	65.42	0.564	0.613	0.608	**0.108**	0.120	**0.084**
	2	136.6	104.2	761.9	9.38	8.02	**62.16**	0.562	0.611	0.610	0.111	0.122	0.088
	3	**136.2**	**103.8**	756	9.58	8.13	65.69	0.560	0.609	0.608	0.108	0.120	0.085
	4	137	105.1	759.3	9.42	8.03	65.83	0.568	0.620	0.615	0.111	0.124	0.086
	5	**137.3**	**105.9**	**767.8**	**9.22**	7.96	64.25	**0.573**	**0.629**	0.625	**0.114**	**0.128**	**0.090**
	6	136.8	105.5	**771.8**	9.44	7.65	**62.39**	0.567	0.619	0.619	0.109	0.125	**0.090**
	7	136.4	104.4	760.2	9.30	7.64	63.51	0.565	0.614	0.613	0.109	0.123	0.087
	8	136.9	104.26	764.01	9.56	8.14	64.51	0.560	0.608	0.605	0.109	0.120	0.086
	9	136.5	104.7	761.4	**9.78**	7.94	64.14	0.557	0.607	0.604	0.108	0.123	0.086
	10	**137.4**	**105.9**	763.8	9.16	7.59	64.47	0.557	0.609	0.604	0.110	0.125	0.086
20 years	11	136.4	104.1	757.1	9.55	8.17	64.60	0.563	0.613	0.609	0.109	0.120	0.085
	12	136.4	104.1	758.7	9.46	8.09	64.23	0.561	0.611	0.609	0.109	0.121	0.086
	13	136.6	104.5	758	9.50	8.11	66.04	0.564	0.615	0.612	0.110	0.122	0.085
	14	137.2	105.5	763.7	9.35	8.01	65.16	0.570	0.625	0.620	**0.112**	0.126	0.087
	15	137.1	105.7	770	9.35	7.84	63.48	0.570	0.624	0.622	0.111	0.126	**0.090**
	16	136.6	105	766.3	9.36	7.66	63.24	0.566	0.617	0.616	0.109	0.124	0.088
	17	136.6	104.4	759	9.40	7.87	64.81	0.562	0.611	0.610	0.109	0.122	0.085
	18	136.9	104.6	759.9	9.54	8.00	65.47	0.559	0.608	0.605	0.109	0.122	0.085
	19	137	105.4	762.6	9.43	7.76	64.55	0.557	0.608	0.604	0.109	0.124	0.086
30 years	20	136.4	104.1	756.8	9.56	8.18	65.29	0.562	0.612	0.609	0.109	0.120	0.085
	21	136.7	104.4	759	9.47	8.12	65.13	0.563	0.614	0.611	0.110	0.122	0.085
	22	136.9	105	761.2	9.42	8.07	65.53	0.567	0.620	0.616	0.111	0.124	0.086
	23	137.1	105.5	766.6	9.38	7.93	64.50	0.569	0.623	0.620	0.111	0.126	0.088
	24	136.9	105.3	766.9	9.33	7.78	63.73	0.568	0.621	0.619	0.111	0.125	0.089
	25	136.7	104.8	763.6	9.40	7.81	64.10	0.564	0.614	0.613	0.109	0.123	0.087
	26	136.7	104.6	760.3	9.35	7.80	64.43	0.560	0.610	0.608	0.110	0.123	0.086
	27	137.1	105.1	761.2	9.40	7.86	65.27	0.558	0.608	0.605	0.110	0.123	0.085
40 years	28	136.6	104.3	757.6	9.54	8.16	65.62	0.564	0.614	0.611	0.109	0.121	0.085
	29	136.8	104.8	761.3	9.42	8.09	64.99	0.566	0.618	0.615	0.111	0.123	0.086
	30	136.9	105.1	764	9.43	7.99	64.94	0.567	0.620	0.617	0.111	0.124	0.087
	31	136.9	105.3	765.1	9.35	7.86	64.44	0.568	0.621	0.618	0.111	0.125	0.088
	32	136.9	105	764.7	9.36	7.86	64.23	0.566	0.618	0.616	0.110	0.124	0.087
	33	136.8	104.9	763.4	9.31	7.71	63.70	0.562	0.612	0.611	0.110	0.124	0.087
	34	136.9	104.9	761.2	9.30	7.75	64.47	0.559	0.609	0.607	0.110	0.123	0.086
50 years	35	136.7	104.7	759.7	9.48	8.13	65.42	0.565	0.617	0.614	0.110	0.122	0.086
	36	136.9	105	763.6	9.42	8.01	64.59	0.566	0.618	0.616	0.111	0.124	0.087
	37	136.8	105	763.3	9.39	7.92	64.80	0.567	0.619	0.616	0.110	0.124	0.087
	38	136.9	105.1	763.7	9.38	7.91	64.69	0.566	0.618	0.616	0.111	0.124	0.087
	39	136.9	105.1	764.4	9.28	7.73	63.63	0.564	0.615	0.613	0.110	0.124	0.088
	40	136.9	105.1	763.6	9.27	7.69	63.84	0.561	0.611	0.609	0.110	0.124	0.087
60 years	41	136.8	104.8	761.8	9.47	8.06	65.02	0.566	0.617	0.615	0.110	0.123	0.086
	42	136.8	104.9	763.1	9.39	7.95	64.49	0.566	0.617	0.615	0.110	0.124	0.087
	43	136.8	104.9	762.5	9.41	7.95	64.95	0.565	0.617	0.614	0.110	0.123	0.086
	44	136.9	105.1	763.5	9.30	7.78	64.03	0.564	0.616	0.613	0.110	0.124	0.087
	45	137	105.2	764.3	9.25	7.71	63.75	0.563	0.614	0.612	0.110	0.125	0.087
70 years	46	136.7	104.8	761.7	9.44	8.00	64.90	0.566	0.617	0.614	0.110	0.123	0.086
	47	136.8	104.8	762.4	9.40	7.97	64.68	0.565	0.616	0.614	0.110	0.123	0.087

(*Continued*)

Extended data Table A2. Continued.

Period		A1			A2			X0			dx		
		Fast	Transitional	Slow	Fast	Transitional	Slow	Fast	Transitional	Slow	Fast	Transitional	Slow
	48	136.8	104.9	762.5	9.34	7.83	64.35	0.564	0.615	0.613	0.110	0.124	0.087
	49	137	105.2	763.6	9.27	7.75	64.03	0.563	0.615	0.612	0.110	0.124	0.087
80 years	50	136.7	104.7	761.2	9.44	8.01	65.02	0.565	0.616	0.613	0.110	0.123	0.086
	51	136.8	104.8	762.3	9.35	7.87	64.20	0.564	0.614	0.612	0.110	0.123	0.087
	52	136.9	105	762.7	9.31	7.80	64.30	0.563	0.614	0.612	0.110	0.124	0.087
90 years	53	136.7	104.7	761.3	9.39	7.92	64.54	0.564	0.614	0.612	0.110	0.123	0.086
	54	136.9	104.9	762.5	9.32	7.83	64.16	0.563	0.614	0.611	0.110	0.124	0.087
100 years	55	136.8	104.8	761.5	9.36	7.88	64.66	0.563	0.614	0.611	0.110	0.123	0.086

Bold numbers are outliers in Extended Data Figure A2.

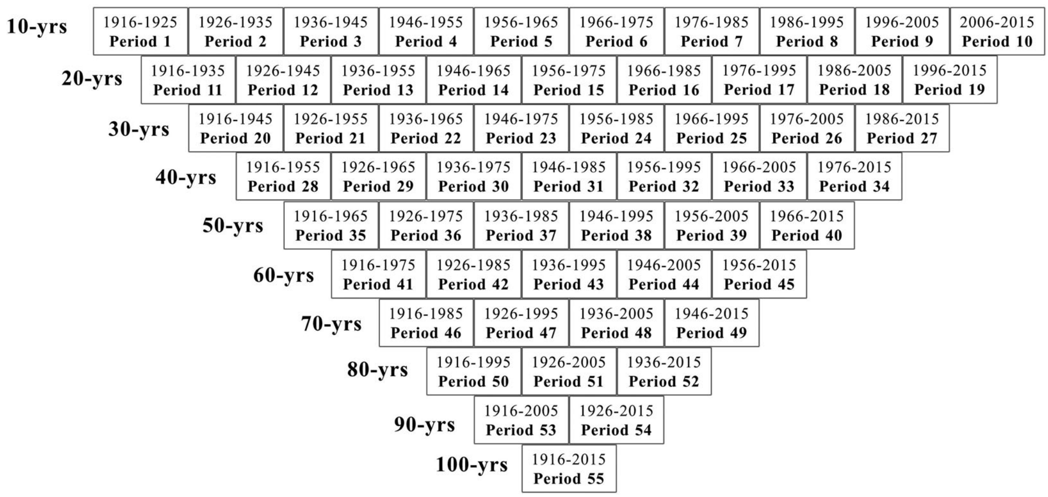

Extended data Figure A1. Grouping of soil organic carbon (SOC) and TD-Index data into 55 subgroups based on different time periods over a span of 100 years (1916–2015)

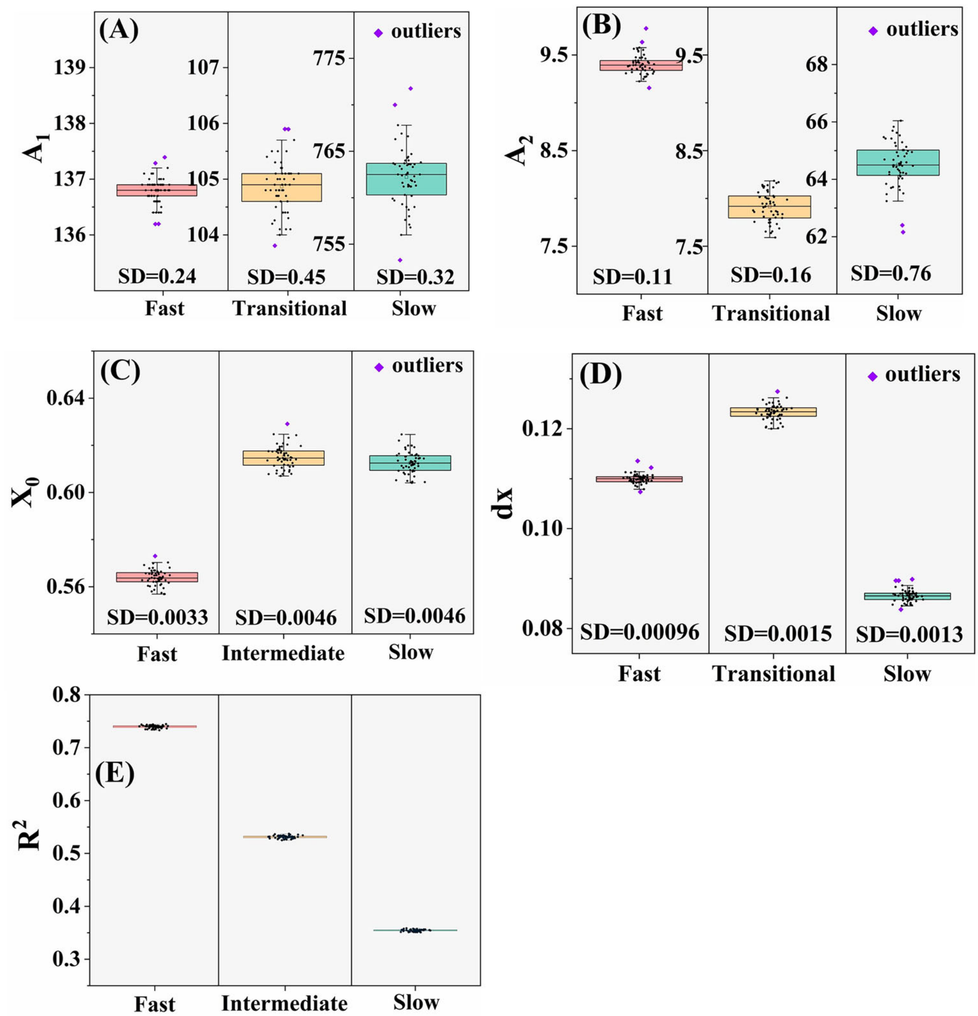

Extended data Figure A2. Time-scale sensitivity of Boltzmann-Sigmoidal Model (BSM) parameters for three soil layers: fast, intermediate, and slow. Each point in the figure represents the parameter value of the BSM model for a specific period. The model was tested using data from 55 different periods to assess its sensitivity to different time scales.

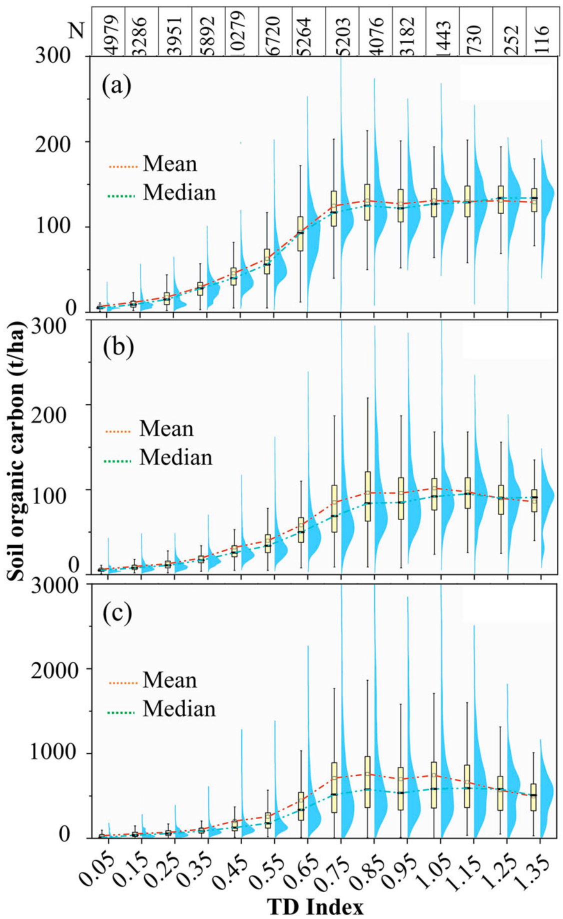

Extended data Figure A3. Distribution and magnitude of soil organic carbon (SOC) in groups with different TD-Index intervals in (a) Fast carbon pool (0–15 cm); (b) Transitional carbon pool (15–30 cm); and (c) Slow carbon pool (30–200 cm). Each 0.5°×0.5° grid point of terrestrial land is divided into a total of 14 groups based on the size of its TD-Index, with each group representing a 0.1 interval. For example, a TD-Index value of 0.05 corresponds to the group within the interval (0, 0.1], while a TD-Index value of 0.15 represents the group within the interval (0.1, 0.2], and so on. *N* denotes the number of grid cells within each group. The red dotted line represents the mean SOC for each group, while the green line represents the median SOC.

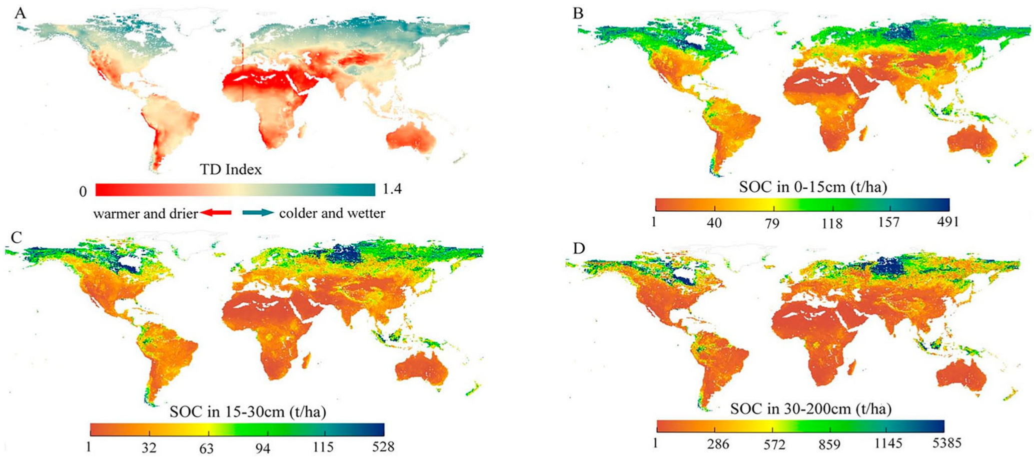

Extended data Figure A4. The global pattern of (A) TD Index, soil organic carbon stock in (B) fast pool (0–15 cm), (C) intermediate pool (15–30 cm) and (D) slow pool (30–200 cm). TD Index defined as exp ($-0.02T-0.8D$), Where T (°C) and D are long-term (1916–2015) annual temperature and dryness. Dryness was defined as Rn/(L*P), where Rn (MJ m^{-2} yr^{-1}) is annual mean net radiation, P (mm yr^{-1}) is and annual mean precipitation, and L (= 2.5 MJ kg^{-1}) is the enthalpy of vaporization.